Available online at website: https://journal.bcrec.id/index.php/bcrec

Bulletin of Chemical Reaction Engineering & Catalysis, 21 (2) 2026, 339-348

Original Research Article

Eco-Friendly Synthesis of ZnO/CQD Photocatalysts from Waste Milk for Myclobutanil Degradation under Visible Light

Hendri Widiyandari[1,2*], Orien Prilita[1], Hanaiyah Parasdila[1], Risa Suryana[1], Osi Arutanti[3]

[1]Department of Physics, Universitas Sebelas Maret, Jl. Ir. Sutami 36 A, Surakarta, Central Java 57126, Indonesia
[2]Centre of Excellence for Electrical Energy Storage Technology, Universitas Sebelas Maret, Jl. Slamet Riyadi 435, Surakarta, Central Java 57146, Indonesia.
[3]Research Center for Chemistry, National Research and Innovation Agency, Tangerang Selatan, Banten 15314, Indonesia.

Received: 9th November 2025; Revised: 4th February 2026; Accepted: 4th February 2026
Available online: 11th February 2026; Published regularly: August 2026

Abstract

Pesticides play a vital role in maintaining the global food supply amid rising agricultural demand and the adverse effects of climate change on crop productivity. Among them, myclobutanil, a triazole-based compound, is commonly used to safeguard plants against fungal diseases. The chemical compounds produced from the high toxicity, mobility, and persistence of pesticides in water can have harmful environmental effects. Food/organic waste has recently gained attention for its potential use in material research, one of them is stale milk. Stale milk contains lactic acid, which can be utilized as a carbon precursor for preparing carbon quantum dot (CQD). In this study, a ZnO/CQD composite photocatalyst was successfully synthesized using CQD derived from stale milk through a green hydrothermal method. The photocatalytic activity of ZnO/CQD in degrading the pesticide myclobutanil was confirmed after 120 min, achieving a degradation efficiency of 30%, while ZnO only 18% under visible light, demonstrating its potential as an excellent photocatalyst candidate for the removal of organic pollutants.

Keywords: Zinc Oxide; Carbon Quantum Dot; Photodegradation; Pesticides; Green Synthesis; Organic Waste

How to Cite: Widiyandari, H., Prilita, O., Parasdila, H., Suryana, R., Arutanti, O. (2026). Eco-Friendly Synthesis of ZnO/CQD Photocatalysts from Waste Milk for Myclobutanil Degradation under Visible Light. *Bulletin of Chemical Reaction Engineering & Catalysis*, 21 (2), 339-348. (DOI: 10.9767/bcrec.20532)

Permalink/DOI: https://doi.org/10.9767/bcrec.20532

1. Introduction

Pesticides are crucial to the global food chain because of the rising demand for agricultural products and the effects of climate change on yields from agriculture [1]. Insect harm, fungus, and weed development that can harm human and environmental health require the usage of pesticides [2]. One type of pesticides used to protect plants from mushrooms is myclobutanil triazole [3]. Chemical compounds resulting from pesticides' high toxicity, mobility, and durability in water have detrimental effects when used [4-5]. Despite significant attempts to control and engineer the use of pesticides, pesticides continue to be found and cause issues in water treatment across the globe [6].

ZnO semiconductors have been investigated recently as excellent sources for resisting bacteria and fungi and as photocatalysts to remove different organic pollutants [7]. ZnO has several advantages, namely its lower cost, resistance to corrosion, a very large bandgap (3.37 eV), and a high exciton binding energy (60 MeV) [8-9]. However, due to the large ZnO band gap, the ZnO semiconductor only exhibits photoactivity when excited by UV light. Additionally, detrimental to ZnO photocatalysis activities is the quick recombination of light-excited electron-hole pairs [10]. Because of this, ZnO material modification as a photocatalyst material still requires optimization.

* Corresponding Author.
Email: hendriwidiyandari@staff.uns.ac.id (H. Widiyandari)

It is possible to modify the material by doping, surface engineering, or combining with other materials to increase light absorption and decrease electron recombination. It can also be composited with carbon material [11–14]. This study introduces ZnO modification through carbon doping to enhance its photocatalytic performance. Carbon acts as an electron reservoir that minimizes electron–hole recombination, while also serving as a photosensitizer that broadens ZnO's light absorption range from the visible to the near-infrared region.

Carbon Quantum Dot (CQD) is nanostructure carbon materials, that has recently received a lot of attention from researchers due to its remarkable features, such as high-water solubility, great photostability, fluorescence, that is dependent on conventional excitation wavelengths, and excellent biocompatibility [15]. In addition, CQD is thought to be helpful in boosting the activity of semiconductor photocatalysts by improving their optics' absorption of visible light in addition to making charge separation easier.

Recent developments in ZnO/CQD heterostructures have shed light on how their photocatalytic efficacy is jointly controlled by band alignment, interfacial electron-transfer routes, and CQD optical sensitization. According to systematic band-structure engineering, well-designed ZnO/CQD interfaces usually adopt a type-II or stepwise alignment, where the CQD LUMO lies slightly above or below the ZnO conduction band. This allows for the efficient extraction of photogenerated electrons from ZnO into CQDs (electron-sink behavior) or the injection of photoexcited electrons from CQDs into ZnO (sensitization mode), both of which suppress charge recombination and extend carrier lifetimes [16]. According to several studies, CQD loading causes significant PL quenching and decreased charge-transfer resistance, which is associated with faster interfacial electron transfer and better e^-/h^+ pair separation. This results in noticeably higher degradation rates or photocurrents when compared to pure ZnO [17].

In addition, CQDs increase solar photon utilization by broadening ZnO's spectral response through strong visible light absorption and, in some formulations, up-conversion photoluminescence, which transforms low-energy visible/NIR photons into higher-energy emission capable of re-exciting ZnO [18,19]. These three combined effects, fast interfacial electron shuttling, band-offset-driven charge separation, and CQD-based sensitization/up-conversio are widely acknowledged as essential design principles in ZnO/CQD photocatalysts of the future [20].

As an environmentally friendly method that can be utilized sustainably for the fabrication of different materials, this study also emphasized the use of green synthesis in the synthesis of CQD. By using natural ingredients, such as plant extracts and biomass waste, as a starting ingredient or reduction agent instead of hazardous chemicals, the CQD green synthesis lowers production costs [21]. Green synthesis was used in this study to create natural precursors for the manufacture of CQD made from stale milk. When employing the hydrothermal process to create highly fluorescent carbon spots that contain nitrogen, milk is a cheap, renewable, and environmentally friendly substance [22].

Therefore, this study aims to develop a green-synthesized ZnO/CQD composite using stale milk-derived carbon quantum dots to enhance visible-light photocatalytic activity for myclobutanil degradation, while elucidating the mechanism of performance improvement through structural and optical analysis.

2. Materials and Method

2.1. Material Synthesis

Trisodium citrate dehydrate (1.47 g) and zinc nitrate hexahydrate (3.72 g) are dissolved in 10 mL of aquades in order to produce ZnO material. Stir at room temperature for 100 min. 1 mL (1 M) of NaOH is gradually added to the solution while it is being stirred until the pH hits 13. The solution is put into the autoclave and heated to 130 ˚C for 10 h once the stirring process is completed. Ethanol and distilled water are used alternately to filter and wash the final products. Additionally, the precipitate is dried at 100 °C for 4 h. then annealed for 3 h at 500 ˚C in order to form a crystal structure.

Carbon Quantum Dot Synthesis from food/organic waste: 10 mL of pure cow's fresh milk are left to stand at room temperature for 4 days. After that, it was placed in the autlocave and heated to 160 ˚C for 3 h. The reaction mixture was allowed to cool to room temperature and subsequently filtered to separate the solid residue from the liquid phase. The resulting CQD filtrate was collected and used directly in the following synthesis steps, yielding approximately 9 mL from an initial 10 mL of precursor solution. For the preparation of the ZnO/CQD composite, 0.2 g of ZnO was dispersed in 45 mL of distilled water and stirred magnetically for 2 h. During the stirring process, 1.5 mL of the CQD solution was introduced dropwise into the suspension to ensure uniform incorporation of the CQDs. The resulting solution of CQD with pH of 4.5 was transferred to a Teflon-lined autoclave and subjected to hydrothermal treatment at 100 °C for 8 h. The obtained products were subsequently filtered and washed thoroughly with ethanol and distilled water. The resulting precipitate was then dried at 100 °C for 4 h.

2.2. Material Characterizations

The synthesized ZnO/CQD were characterized using XRD (X-Ray Diffraction), TEM (Transmission Electron Microscopy), UV-Vis DRS (Ultraviolet-Visible Diffuse Reflectance Spectroscopy), UV-Vis spectrometer, FE-SEM/EDX (Field Emission Scanning Electron Microscopy/Energy Dispersive X-ray Spectroscopy). To determine the shape of the crystal structure produced during the synthesis process, the XRD test (XRD, Rigaku Smartlab, Japan) using Cu K ∝ radiation (λ= 1.5406Å) in the range of 10–90° is used. In order to determine the sample's morphological form, elemental composition, and particle dispersion in the sample, the FE-SEM/EDX (FE-SEM/EDX, JEOL JIB-4610F, Japan) test is being used, High-resolution transmission electron microscopy (HRTEM, JFIB 4610F, Japan) is used to directly image and determine the atomic structure, crystalline lattice, and atomic arrangements of materials. UV-Vis DRS (Shimadzu, Japan) to determine the subsequent band gap energy that is achieved.

2.3. Photocatalytic Activity Testing

Photodegradation is used to test photocatalytic activity by dissolving up to 0.1 g of ZnO/CQD in a 30 ppm (50 mL) solution of the pesticide myclobutanil. The test lasted 150 min, of which the first 30 were spent in the absence of radiation and the remaining 120 were spent under visible light Xe lamp illumination without any cut-off filter (Solar Simulator, Peccel/Pec-L01, 1000 W/m^2 which roughly corresponds to 100000 lux by illuminator). To separate the photocatalyst powder and pesticide solution, the sample was centrifuged for 20 min at 5000 rpm following photodegradation. Additionally, the UV-Vis spectrometer measures the pesticide solution's absorbance value.

3. Results and Discussion

3.1. Characterizations

The UV-VIS spectrum of CQD and the graph in Figure 1 show the CQD solution under UV irradiation (right) and without UV irradiation (left). The absorption spectrum of CQD has a broad band between 250 and 600 nm, indicating the presence of π-π* and n-π* transitions, which can be attributed to C=C and C=O bonds [23]. The images of the CQD solution were taken at a wavelength of 365 nm under UV irradiation and without UV irradiation; the images appeared transparent without UV irradiation but emitted a clear blue light under UV irradiation. This occurs as a result of some electrons being excited to higher energy states [24].

The characterisation of X-ray diffraction can be used to determine the crystal structure. The ZnO and ZnO/CQD XRD patterns are displayed in Figure 2. Both ZnO and ZnO/CQD exhibit identical diffraction peaks corresponding to the wurtzite ZnO crystal planes (100), (002), (101), (102), (110), and (103), located at 2θ = 32.15°, 34.38°, 36.22°, 47.49°, 56.54°, and 62.78°, respectively. The matching peak positions and intensities indicate that the incorporation of CQDs does not alter the crystalline phase or structural framework of ZnO. Table 1 shows the calculation of crystal size using the Scherrer equation (Equation (1)) and the lattice parameter of the ZnO and ZnO/CQD. A slight decrease in crystallite size from 29.4 nm to 28.4 nm indicates minor suppression of grain growth due to surface interactions between CQDs and ZnO during nucleation. The lattice parameters (a and c) and the c/a ratio remain essentially unchanged, demonstrating that CQDs do not enter the ZnO lattice and induce only negligible lattice strain. Overall, the structural analysis suggests that the influence of CQDs is confined to surface-level effects while the wurtzite framework remains

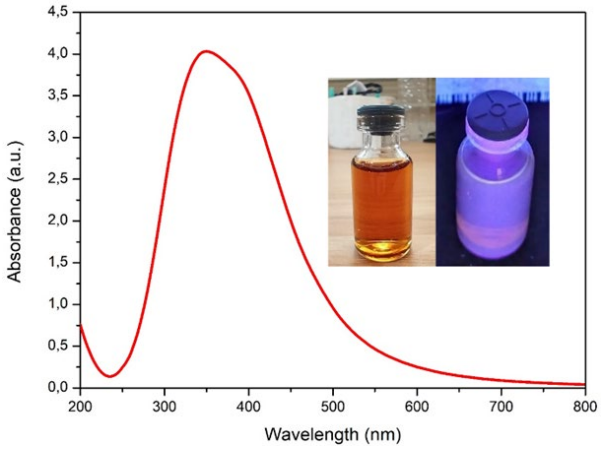

Figure 1. UV-Vis absorbtion spectra of CQDs, and digital photograph of CQDs solution without (left) and with (right) UV irradiation.

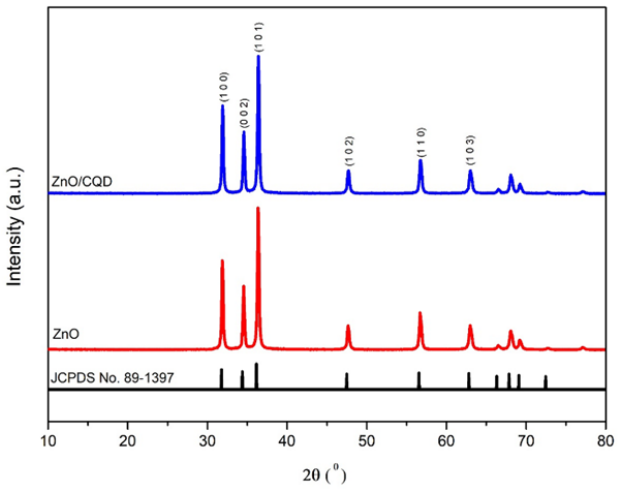

Figure 2. Diffraction pattern of ZnO and ZnO/CQD.

intact. Furthermore, the low crystallinity structure due to the CQD concentration in ZnO/CQD result in an XRD pattern that is comparable to that of ZnO [25].

$$D = \frac{k\lambda}{\beta \cos\theta} \quad (1)$$

where, D = size of crystal diameter, λ = wave-length of radiation, θ = angle of diffraction of Bragg, β = width of peak FWHM, k = constant (0,9) [26].

Figure 3 displays the results of the SEM test for ZnO morphology. Low magnification SEM is shown in Figure 3 (a) and (b), whereas high magnification SEM is shown in Figure 3 (c) and (d). The hexagonal nanorod structure of ZnO and ZnO/CQD materials distributes evenly. Figure 3(e) and (f) each material's average particle size is 453.94 nm for ZnO and 413 nm for ZnO/CQD. Therefore, the average particle size may be impacted by the presence of CQD on the ZnO surface. Energy dispersive X-ray spectroscopy (EDX) (Figure 3 (g-i)) revealed the presence of C, Zn, and O as the main elements in the nanocomposite. The weight percentage and atomic percentage of each element of all components based on the EDX study are summarized in Table 2. Interestingly, the C content in the ZnO/CQD nanocomposite was determined through EDX analysis to be 13.3%.

The presence of CQD is detected by HR-TEM. The grid linea of the ZnO/CQD lattice and the grid's distance value of 0.19 nm are visible in Figure 4(a), which displays the HR-TEM of ZnO/CQD particles made using hydrothermal methods. SAED pattern of the ZnO/CQD material shown in Figure 4(b) exhibits clear

Table 1. XRD data of ZnO/CQD preferred (101) crystal plane.

Sampel	2θ	FWHM	Crystallite Size (nm)	a (Å)	c (Å)	c/a
ZnO	36.22	0.67062	29.385	2.849	4.935	1.7320
ZnO/CQD	36.22	0.59796	28.389	2.848	4.932	1.7321

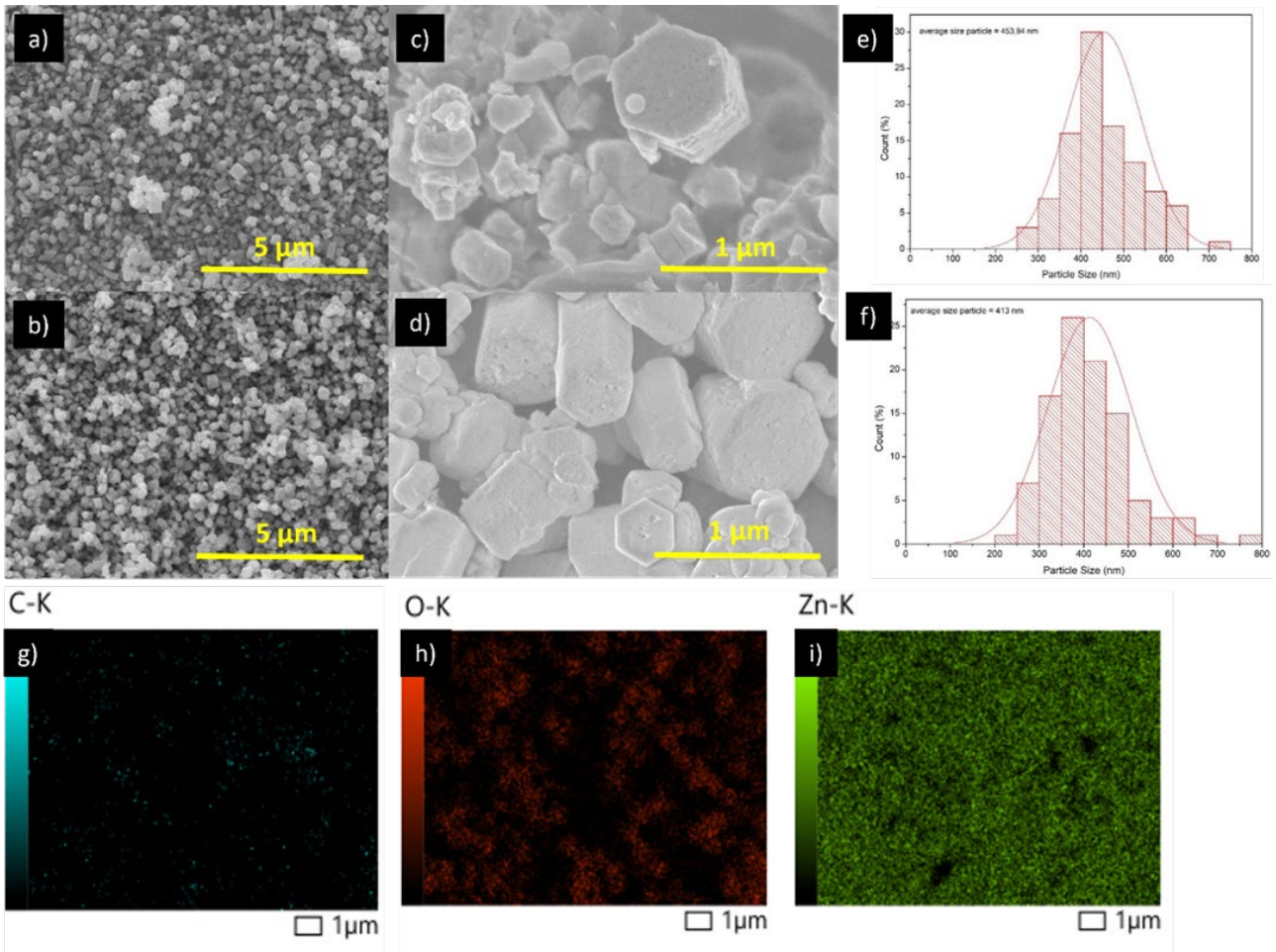

Figure 3. (a) Low Magnification FE-SEM of ZnO, (b) Low Magnification FE-SEM of ZnO/CQD, (c) High Magnification FE-SEM of ZnO, (d) High Magnification FE-SEM of ZnO/CQD, particle size distribution of (e) ZnO and (f) ZnO/CQD, and (g-i) Element mapping of ZnO/CQD.

diffraction rings, indicating the single crystalline nature of the ZnO/CQD.

3.2 Photocatalytic Activities

The top of the emission curve in the PL spectrum seen in Figure 5 lies between 545 and 575 nm. In comparison to ZnO, the ZnO/CQD peak's PL emission intensity decreased. This can be explained by the fact that CQD functions as an electron acceptor, which can lower the intensity of photoluminescence and increase the response of the transient of ZnO copying. In other words, by separating the electron-hole pair, CQD can boost photocatalytic activity and improve light absorption in the visible light spectrum [27].

The PL spectra of pure ZnO and ZnO/CQD (Figure 5) exhibit a strong UV emission band centered at ~280 nm, which is associated with the near-band-edge recombination of excitons in ZnO. Notably, the PL intensity of the ZnO/CQD sample is significantly lower than that of bare ZnO. This pronounced quenching indicates a reduced radiative recombination probability of photogenerated electron–hole pairs, suggesting more efficient charge separation in the presence of CQDs. The CQDs act as additional electron-accepting sites at the ZnO surface, providing alternative non-radiative pathways and facilitating interfacial charge transfer. As a result, more electrons and holes are available to participate in redox reactions with adsorbed species (e.g., O_2 and H_2O), leading to enhanced generation of reactive oxygen species and, consequently, improved photocatalytic activity compared with pristine ZnO.

A crucial approach to analyzing photocatalytic reactions to the degradation process is the analysis of band gaps. The band gaps of ZnO and ZnO/CQD were determined using diffuse reflectance UV–Vis spectroscopy. Figure 6 presents the corresponding Tauc plots, constructed assuming a direct allowed transition consistent with the wurtzite ZnO electronic structure. The results show that the incorporation of CQD induces a slight reduction in the band gap, decreasing from 2.93 eV for pristine ZnO to 2.86 eV for the ZnO/CQD composite. These findings clarify how adding CQD can expand the region of light absorption and thus boost visible light's catalytic potential [28]. Based on previous study, Yashwant *et al*. [29], they analyzed NS-CDOTs and ZnO nanorods by using Mott-Schottky in order to better understand the reciprocal advantages of NS-CDOTs and ZnO nanorods, as well as to learn more about the band structure and charge transfer process. the findings stated that the conduction band (CB)of NS-CDOTs is

Table 2. Percentage of elements contained in the material.

Elements	ZnO		ZnO/CQD	
	Mass%	Atom%	Mass%	Atom%
Zn	76.97	55.00	75.73	39.32
O	23.03	45.00	11.24	23.85
C	-	-	13.03	36.83

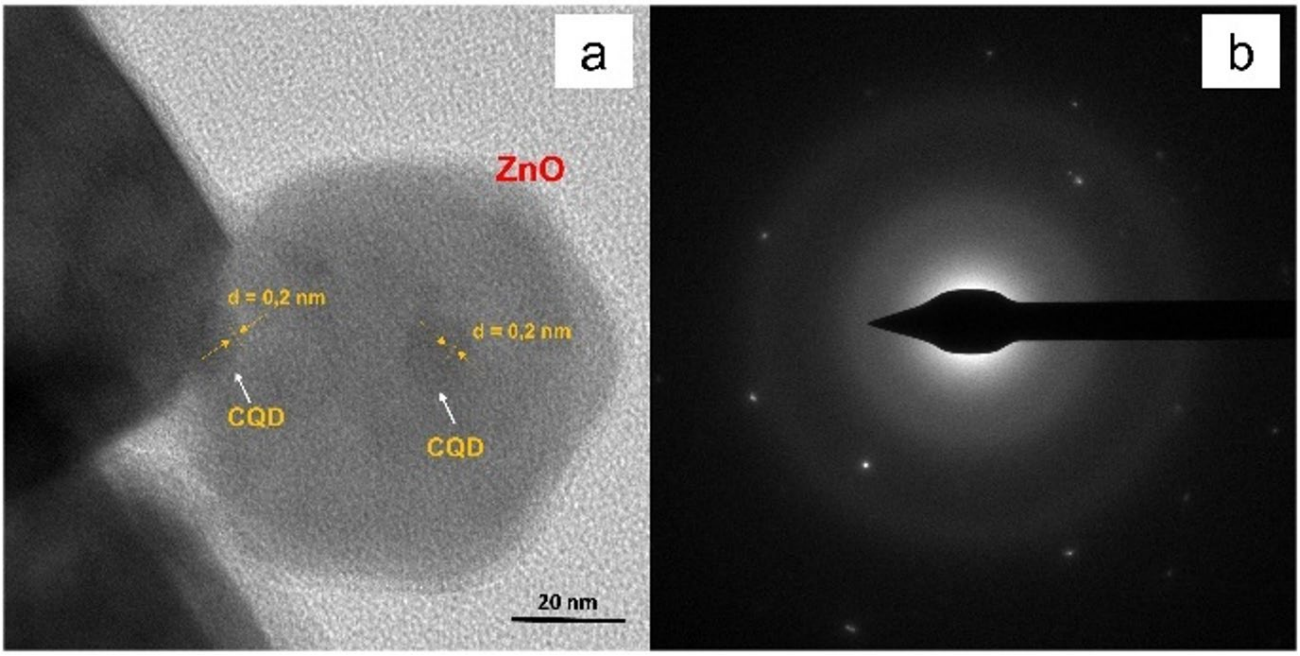

Figure 4. (a) HR-TEM image of ZnO/CQD and (b) Selected Area Electron Diffraction (SAED) pattern.

greater than that of ZnO, which favors thetransfer of electrons from the CB of NS-CDOTs to the CB of ZnO. Further, The valence band (VB) of NS-CDOTs and ZnO is found to be in the range 1.74 eV and 3.1 eV (Vs NHE), respectively.

Figure 7 presents the UV–Vis spectra of myclobutanil degradation under visible-light irradiation in the presence of (a) ZnO, (b) ZnO/CQDs, and without a photocatalyst (c), recorded at different irradiation times. In all cases, the characteristic absorption band of myclobutanil in the 215–230 nm region decreases with irradiation time, indicating molecular degradation. For bare ZnO, the absorbance shows a non-monotonic change at the early stage, suggesting limited visible-light activity and the possible formation of transient intermediates. In contrast, the ZnO/CQDs composite exhibits a clear and continuous decrease in absorbance over time, demonstrating enhanced and more stable photocatalytic performance under visible light, attributed to improved light harvesting and charge separation by CQDs. Meanwhile, the catalyst-free system shows only weak and

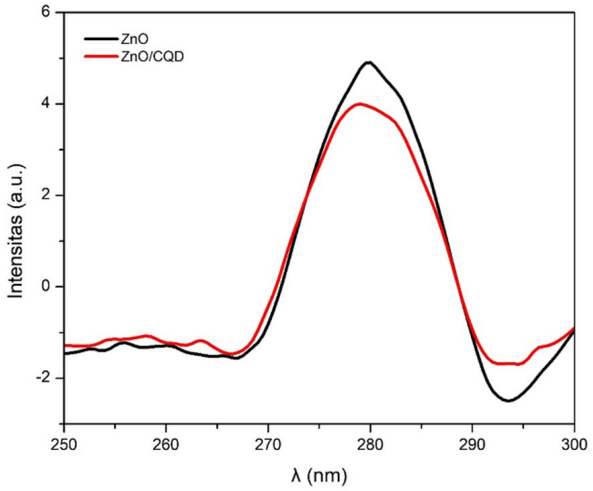

Figure 5. PL spectra of ZnO and ZnO/CQD.

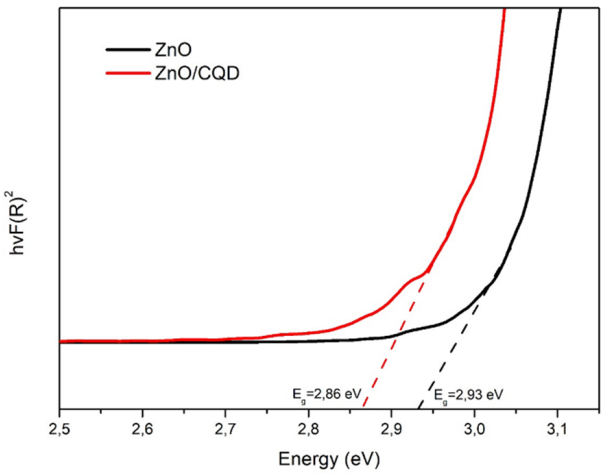

Figure 6. Band gap energy of ZnO and ZnO/CQD.

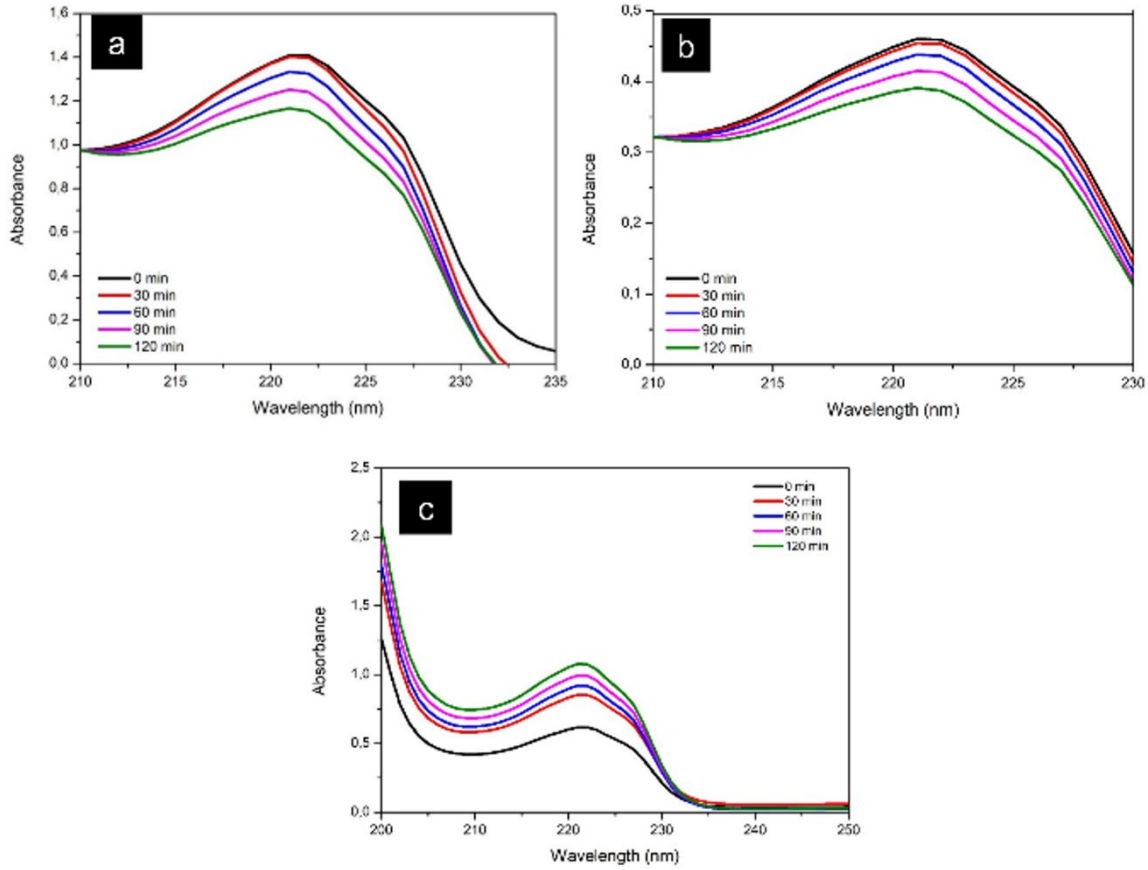

Figure 7. UV–visible absorption spectra for degradation of myclobutanil pesticide on (a) ZnO, (b) ZnO/CQD, (c) without photocatalyst, under visible light irradiation.

unstable absorbance changes, confirming that direct photolysis under visible light isnefficient compared to photocatalytic processes.

Figure 8(a) shows the percentage degradation of myclobutanil over ZnO, ZnO/CQD, and in the absence of a photocatalyst (negative control). It is evident that ZnO/CQD degrades myclobutanil more rapidly than pristine ZnO. Based on the degradation percentage calculated using Equation (2), ZnO/CQD achieves approximately 30% degradation after 120 min of irradiation, whereas pristine ZnO exhibits a significantly lower efficiency, with only about 18% degradation observed under the same conditions. The degradation percentage equation [30]:

$$Degradation\ (\%) = \frac{C_0 - C}{C} \times 100\% \quad (2)$$

where C_0 is the initial concentration at $t = 0$ and C is the concentration of the pollutant at a given irradiation time. Compared to ZnO, the myclobutanil concentration decreases more rapidly in the presence of ZnO/CQD, indicating that the incorporation of CQDs enhances the photocatalytic performance of ZnO by improving charge separation and extending the light absorption range. Compared to ZnO, the concentration of myclobutanil pesticides decreases more quickly in ZnO/CQD material. This phenomenom explains how adding CQD can improve ZnO photocatalytic activity performance and the spectrum of light absorption.

The partial photodegradation of myclobutanil (~30–40% after 2 h irradiation) nonetheless provides measurable environmental benefits. First, reducing parent compound concentration proportionally decreases acute and chronic toxicity, especially considering the nonlinear toxic response of aquatic microorganisms to triazole fungicides [31]. Second, photolytic cleavage produces more polar, less persistent intermediates that are more amenable to subsequent biotic degradation, thus accelerating natural environmental attenuation [32]. Third, lower concentrations in the aqueous phase reduce the potential for bioaccumulation and long-range mobilization [33]. Consequently, even partial photodegradation plays an important role in mitigating the persistence, mobility, and ecological risk associated with myclobutanil contamination.

Figure 8 (b) shows the ln C/C_0 vs time curves of the ZnO, ZnO/CQD, and negative control, where the slope denotes the constant rate of the photocatalytic activity reaction (K). The first-order reaction kinetics during the degradation process are represented by linear regression (R^2). According to these findings, the photodegradation of the myclobutanil pesticide in photocatalyst confirms to the kinetics of the first order reaction and the Hinshelwood Langmuir (L-H) Kinetics model [34]:

$$\ln\left(\frac{C_0}{C_t}\right) = k_c t \quad (3)$$

As shown in Table 3, ZnO/CQD has a linear regression value (R^2) of 0.8624. Table 3 shows that the reaction rates for ZnO and ZnO/CQD are both constant at -0.00173 min^{-1} and -0.00264 min^{-1}. The decrease in pesticide concentration in each subsequent cycle is shown in Figure 8(c). The reusability results show relatively stable pesticide degradation, with 25% efficiency in cycle 1 and increasing to 26% in cycle 2, indicating that the material remains active after reuse.

Table 3. Kinetic rate of myclobutanil pesticide reaction.

Sample	R^2	K (min^{-1})
ZnO	0.9246	-0.00173
ZnO/CQD	0.8624	-0.00264
Negative Control	0.8258	0.0042

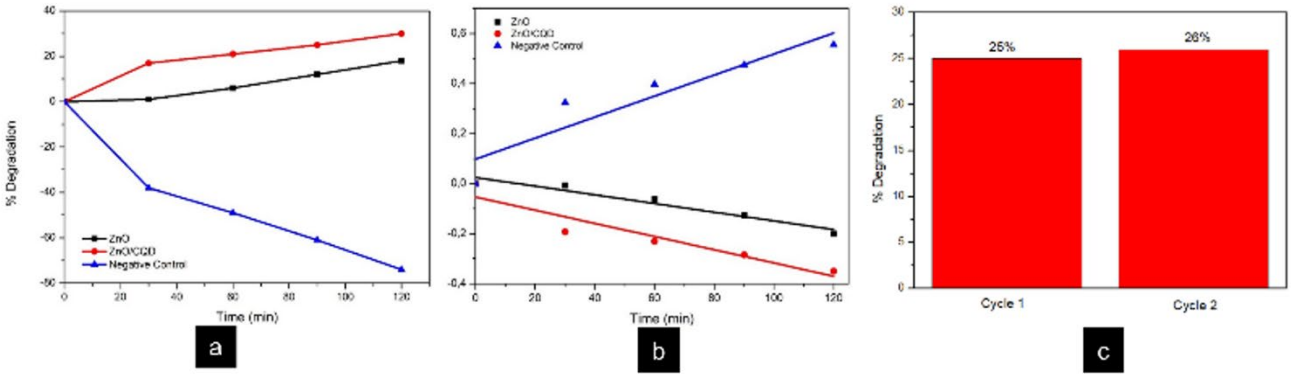

Figure 8. (a) Concentration of degradation, (b) the pseudo-first-order kinetic of Langmuir-Hinshelwood (L–H) curves of the ZnO, ZnO/CQD, and negative control, (c) Reusability of ZnO/CQD sample for the photodegradation of myclobutanil pesticide after 120 min irradiation.

4. Conclusions

Stale milk was successfully utilized as a sustainable carbon precursor in the green synthesis of carbon quantum dot (CQD). The incorporation of CQD significantly modified the structural and optical properties of ZnO, reducing its bandgap to 2.86 eV and thereby extending its photocatalytic response into the visible-light region while suppressing rapid electron–hole recombination. The resulting ZnO/CQD composite exhibited enhanced photocatalytic activity, achieving approximately 30% degradation of myclobutanil pesticide within 120 min. These results demonstrate that CQD incorporation effectively improves the photocatalytic performance of ZnO.

Acknowledgment

This research was financially supported by Universitas Sebelas Maret under the Scheme of PKGR-UNS (Grant Number 371/UN27.22/PT.01.03/2025).

CRedit Author Statement

Author Contributions: H. W.: Validation, Supervision, Project administration, Methodology, Conceptualization, and Funding acquisition. O. P.: Writing – original draft, Investigation, Data Curation, and Visualization. H. P.: Writing – original draft, Writing – review & editing, Validation, Formal analysis. R. S.: Validation and Supervision. All authors have read and agreed to the published version of the manuscript.

References

[1] Wuepper, D., Tang, F.H., Finger, R. (2023). National leverage points to reduce global pesticide pollution. *Global Environmental Change*, *78*, 102631. DOI: 10.1016/j.gloenvcha.2022.102631

[2] Albaseer, S.S. (2019). Factors controlling the fate of pyrethroids residues during post-harvest processing of raw agricultural crops: an overview. *Food chemistry*, *295*, 58-63. DOI: 10.1016/j.foodchem.2019.05.109

[3] Roman, D.L., Matica, M.A., Ciorsac, A., Boros, B.V., Isvoran, A. (2023). The effects of the fungicide myclobutanil on soil enzyme activity. *Agriculture*, *13*(10), 1956. DOI: 10.3390/agriculture13101956

[4] Fiorenza, R., Di Mauro, A., Cantarella, M., Iaria, C., Scalisi, E.M., Brundo, M.V., ... Impellizzeri, G. (2020). Preferential removal of pesticides from water by molecular imprinting on TiO2 photocatalysts. *Chemical Engineering Journal*, *379*, 122309. DOI: 10.1016/j.cej.2019.122309

[5] Vaya, D., Surolia, P.K. (2020). Semiconductor based photocatalytic degradation of pesticides: An overview. *Environmental Technology & Innovation*, *20*, 101128. DOI: 10.1016/j.eti.2020.101128

[6] Kanan, S., Moyet, M.A., Arthur, R.B., Patterson, H.H. (2020). Recent advances on TiO2-based photocatalysts toward the degradation of pesticides and major organic pollutants from water bodies. *Catalysis Reviews*, *62*(1), 1-65. DOI: 10.1080/01614940.2019.1613323

[7] Poongodi, G., Anandan, P., Kumar, R.M., Jayavel, R. (2015). Studies on visible light photocatalytic and antibacterial activities of nanostructured cobalt doped ZnO thin films prepared by sol–gel spin coating method. *Spectrochimica Acta Part A: Molecular and Biomolecular Spectroscopy*, *148*, 237-243. DOI: 10.1016/j.saa.2015.03.134

[8] Raha, S., Ahmaruzzaman, Md. (2022). ZnO nanostructured materials and their potential applications: progress, challenges and perspectives. *Nanoscale Advances*, 4(8), 1868–1925. DOI: 10.1039/d1na00880c

[9] Baruah, S., Dutta, J. (2009). Hydrothermal growth of ZnO nanostructures. *Science and Technology of Advanced Materials*, *10*(1), 013001. DOI: 10.1088/1468-6996/10/1/013001

[10] Xie, W., Li, Y., Sun, W., Huang, J., Xie, H., Zhao, X. (2010). Surface modification of ZnO with Ag improves its photocatalytic efficiency and photostability. *Journal of Photochemistry and Photobiology A: Chemistry*, *216*(2-3), 149-155. DOI: 10.1016/j.jphotochem.2010.06.032

[11] Ore, O.T., Adeola, A.O., Bayode, A.A., Adedipe, D.T., Nomngongo, P.N. (2023). Organophosphate pesticide residues in environmental and biological matrices: Occurrence, distribution and potential remedial approaches. *Environmental Chemistry and Ecotoxicology*, *5*, 9-23. DOI: 10.1016/j.enceco.2022.10.004

[12] Roza, L., Fauzia, V., Rahman, M.Y.A., Isnaeni, I., Putro, P.A. (2020). ZnO nanorods decorated with carbon nanodots and its metal doping as efficient photocatalyst for degradation of methyl blue solution. *Optical Materials*, *109*, 110360. DOI: 10.1016/j.optmat.2020.110360

[13] Thakur, S., Bains, A., Sridhar, K., Kaushik, R., Chawla, P., Sharma, M. (2023). Valorization of food industrial waste: Green synthesis of carbon quantum dots and novel applications. *Chemosphere*, 140656. DOI: 10.1016/j.chemosphere.2023.140656

[14] Koutamehr, M.E., Moradi, M., Tajik, H., Molaei, R., Heshmati, M.K., Alizadeh, A. (2023). Sour whey-derived carbon dots; synthesis, characterization, antioxidant activity and antimicrobial performance on foodborne pathogens. *LWT*, *184*, 114978. DOI: 10.1016/j.lwt.2023.114978

[15] Arumugam, S.S., Xuing, J., Viswadevarayalu, A., Rong, Y., Sabarinathan, D., Ali, S., Chen, Q. (2020). Facile preparation of fluorescent carbon quantum dots from denatured sour milk and its multifunctional applications in the fluorometric determination of gold ions, in vitro bioimaging and fluorescent polymer film. *Journal of Photochemistry and Photobiology A: Chemistry*, *401*, 112788. DOI: 10.1016/j.jphotochem.2020.112788

[16] Jung, H., Sapner, V.S., Adhikari, A., Sathe, B.R., Patel, R. (2022). Recent Progress on Carbon Quantum Dots Based Photocatalysis. *Frontiers in Chemistry*, 10. DOI: 10.3389/fchem.2022.881495

[17] Toma, E.E., Stoian, G., Cojocaru, B., Parvulescu, V.I., Coman, S.M. (2022). ZnO/CQDs Nanocomposites for Visible Light Photodegradation of Organic Pollutants. *Catalysts*, 12(9), 952. DOI: 10.3390/catal12090952

[18] Bansal, H., Sethi, P., Basu, S. (2025). Nanoflower-like ZnO–carbon quantum dot heterostructures for solar-driven degradation of methylene blue: a high-performance and recyclable photocatalyst for sustainable wastewater treatment. *Materials Advances*, 6(20), 7585–7598. DOI: 10.1039/d5ma00804b

[19] Sinha, R., Roy, N., Mandal, T.K. (2023). N-Doped Carbon Dots and ZnO Conglomerated Electrodes for Optically Responsive Supercapacitor Applications. *Langmuir*, 39(12), 4518–4529. DOI: 10.1021/acs.langmuir.3c00300

[20] Nadikatla, S. K., Chintada, V. B., Gurugubelli, T. R., & Koutavarapu, R. (2023). Review of Recent Developments in the Fabrication of ZnO/CdS Heterostructure Photocatalysts for Degradation of Organic Pollutants and Hydrogen Production. *Molecules*, 28(11), 4277. DOI: 10.3390/molecules28114277

[21] Fan, H., Zhang, M., Bhandari, B., Yang, C.H. (2020). Food waste as a carbon source in carbon quantum dots technology and their applications in food safety detection. *Trends in Food Science & Technology*, 95, 86-96. DOI: 10.1016/j.tifs.2019.11.008

[22] Wang, L., Zhou, H.S. (2014). Green synthesis of luminescent nitrogen-doped carbon dots from milk and its imaging application. *Analytical chemistry*, *86*(18), 8902-8905. DOI: 10.1021/ac502646x

[23] Lin, C., Dong, B., Xu, Z. (2023). A value product after the hydrothermal treatment of sludge: Carbon quantum dots and its application. *Journal of Environmental Chemical Engineering*, *11*(6), 111430. DOI: 10.1016/j.jece.2023.111430

[24] Abd Rani, U., Ng, L.Y., Ng, C.Y., Mahmoudi, E. (2020). A review of carbon quantum dots and their applications in wastewater treatment. *Advances in colloid and interface science*, *278*, 102124. DOI: 10.1016/j.cis.2020.102124

[25] Bozetine, H., Wang, Q., Barras, A., Li, M., Hadjersi, T., Szunerits, S., Boukherroub, R. (2016). Green chemistry approach for the synthesis of ZnO–carbon dots nanocomposites with good photocatalytic properties under visible light. *Journal of Colloid and Interface Science*, *465*, 286-294. DOI: 10.1016/j.jcis.2015.12.001

[26] Widiyandari, H., Nashir, M., Parasdila, H., Almas, K.F., Suryana, R. (2023). Ag-TiO2 For Efficient Methylene Blue Photodegradation Under Visible Light Irradiation. *Bulletin Of Chemical Reaction Engineering & Catalysis*, *18*(4), 593-603. DOI: 10.9767/bcrec.19885

[27] Gao, D., Zhao, P., Lyu, B., Li, Y., Hou, Y., Ma, J. (2020). Carbon quantum dots decorated on ZnO nanoparticles: An efficient visible-light responsive antibacterial agents. *Applied Organometallic Chemistry*, *34*(8), e5665. DOI: 10.1002/aoc.5665

[28] Le, S., Li, W., Wang, Y., Jiang, X., Yang, X., Wang, X. (2019). Carbon dots sensitized 2D-2D heterojunction of BiVO4/Bi3TaO7 for visible light photocatalytic removal towards the broad-spectrum antibiotics. *Journal of hazardous materials*, *376*, 1-11. DOI: 10.1016/j.jhazmat.2019.04.088

[29] Yashwanth, H.J., Naik, M.M., Udayabhanu, U., Kumar, M.P., Vinuth, M., Dileep, M.S. (2025). Enhanced photocatalytic hydrogen evolution via nitrogen and sulfur Co-functionalized carbon quantum Dot-Modified ZnO nanocomposites: experimental insights and mechanistic Understanding. J*ournal of Environmental Chemical Engineering*, 119249. DOI: 10.1016/j.jece.2025.119249

[30] Al Haiqi, O., Nour, A.H., Bargaa, R., Ayodele, B.V. (2020). Effect of Process Parameters on the Photocatalytic Degradation of Phenol in Oilfield Produced Wastewater using ZnO/Fe2O3 Nanocomposites. *Bulletin of Chemical Reaction Engineering & Catalysis*, *15*(1), 128-136. DOI: 10.9767/bcrec.15.1.6068.128-136

[31] Liu, W.-R., Ying, G.-G., Zhao, J.-L., Liu, Y.-S., Hu, L.-X., Yao, L., Liang, Y.-Q., Tian, F. (2016). Photodegradation of the azole fungicide climbazole by ultraviolet irradiation under different conditions: Kinetics, mechanism and toxicity evaluation. *Journal of Hazardous Materials*, 318, 794–801. DOI: 10.1016/j.jhazmat.2016.06.033

[32] Yuan, Y., Li, D., Huang, H., He, J., Yu, C., Gao, Y., Vione, D., Fang, H. (2025). Direct photodegradation of aromatic carbamate pesticides: Kinetics and mechanisms in aqueous vs. non-aqueous media. *Journal of Hazardous Materials*, 489, 137648. DOI: 10.1016/j.jhazmat.2025.137648

[33] Garcia-Muñoz, P., Dachtler, W., Altmayer, B., Schulz, R., Robert, D., Seitz, F., Rosenfeldt, R., Keller, N. (2020). Reaction pathways, kinetics and toxicity assessment during the photocatalytic degradation of glyphosate and myclobutanil pesticides: Influence of the aqueous matrix. *Chemical Engineering Journal*, 384, 123315. DOI: 10.1016/j.cej.2019.123315

[34] Samad, M.A.B., Quayum, E., Hossain, M.A., Islam, T.S., Khan, M.M.R. (2023). Synthesis and Characterization of TiO2-ZnO Nanocomposite Photocatalyst for the Removal of Basic Violet 14 as an Industrial Dye. *Bulletin of Chemical Reaction Engineering & Catalysis*, *18*(4), 688-699. DOI: 10.9767/bcrec.20059.